Prod. Eng. Res. Devel. (2011) 5:17–24
DOI 10.1007/s11740-010-0275-9

PRODUCTION PROCESS

The preparation of cutting edges using a marking laser

J. C. Aurich · M. Zimmermann · L. Leitz

Received: 13 July 2010 / Accepted: 9 September 2010 / Published online: 23 September 2010

Abstract During the machining process, high mechanical and thermal loads occur at the cutting edge. Such loads can cause tool failure. Specifically non-uniform and sharp cutting edges that have a low cutting edge stability lead to such failures. In order to enhance the tool performance, the cutting edges are prepared by manufacturing both a predefined cutting edge geometry, and an appropriate cutting edge roughness. This paper describes the use of a low-cost marking laser for the preparation of cutting edges as an alternative to conventional preparation techniques, such as brushing or blasting. Cutting edge radii of 9–47 μm can be prepared with a machining accuracy of 1.5 μm. The maximum preparation time for an individual cutting edge is approximately 10 s. Uncoated indexable inserts manufactured in this way were tested in a face milling operation. The results of these investigations (using prepared cutting edges) show both an increase in tool life and an improved surface roughness of the machined workpieces compared to those using non-prepared cutting edges.

Keywords Cutting edge · Cutting edge preparation · Laser · Milling

1 Introduction

Optimization of cutting tools has previously been achieved mainly by improving the cutting material, the coating system and the tool macro geometry. The increasing demand on cutting tools with regards to the material removal rates, the chip removal of hard-to-machine materials, and the tool life, require further substantial optimization. These can be achieved through the use of enhanced tool micro geometry using cutting edge preparation [1]. The preparation of cutting edges ensures both a uniform cutting edge and a defined cutting edge geometry. Using such a process, the tool performance can be significantly increased [2, 3].

For the modification of the cutting edge micro geometry, the most common processes are blasting or brushing [4, 5]. Blasting is used for the preparation of the cutting edges, as well as mechanical pre-treatment of the tool surfaces prior to coating. Brushing techniques are restricted to the preparation of cutting edges [5]. By using these described processes certain disadvantages such as residues on the cutting edge, low processing speeds and limitations concerning the reproducible achievable cutting edge micro geometry have to be accepted [7–9].

A promising alternative for the preparation of cutting edges is laser machining. It has been demonstrated that the preparation of cutting edges using laser radiation is a useful improvement compared to the use of conventional preparation technologies. High cutting edge quality has been achieved through the use of frequency-converted diode-pumped solid-state lasers [6]. However, lasers with pulse durations of approximately 12 ps incur very high costs. Therefore, a low-cost marking laser was used to investigate the capability of such lasers for cutting edge preparation.

2 Cutting edge specification

For the evaluation of the cutting edge micro-geometry it is necessary to use consistent specifications. The cutting edge

J. C. Aurich · M. Zimmermann (✉) · L. Leitz
Institute for Manufacturing Technology and Production Systems, University of Kaiserslautern, Kaiserslautern, Rhineland-Palatinate, Germany
e-mail: zimmermann@cpk.uni-kl.de
URL: www.fbk-kl.de

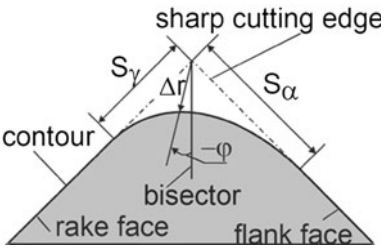

Fig. 1 Characterization of the cutting edge micro geometry [10]

micro geometry is often defined by the cutting edge radius $r_ß$. Denkena [10] proposed four new characterization parameters: Δr, φ, S_γ, S_α (Fig. 1). These parameters ensure a detailed description of uneven cutting edge shapes.

The value Δr describes the distance between the maximum point of the cutting edge contour and the theoretical intersection point of the sharp cutting edge. The angle φ specifies the shift of the cut point either to the rake face—or to the flank face, S_γ and S_α describe the sharp or obtuse run of the curve to the rake face, or the flank-face, respectively [10].

3 Laser preparation of cutting edges

The preparation of the cutting edge was conducted using a diode-pumped solid state laser (Nd:YVO_4). The laser beam has a Gaussian energy distribution across the spot diameter. This energy distribution ensures a smooth transition between the laser processed area and the area without laser processing. The laser system (Fig. 2) operates in a pulse wave mode. This allows for both improved surface integrity, and a rising amount of ablated material compared to the use of a continuous wave mode. The increased efficiency of material ablation can be attributed to the significantly higher amount of deposited energy per unit area compared to the use of continuous wave mode. Improved surface integrity can be achieved by the use of short laser pulses. In such cases, the laser pulse hits the workpiece and the surface is first heated to its melting point and then to its evaporation point. For long pulse durations a large

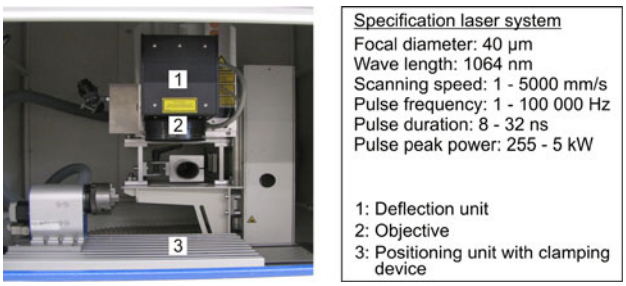

Fig. 2 Laser system

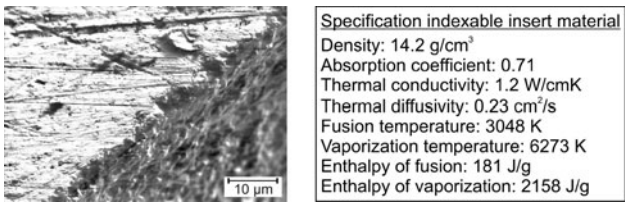

Fig. 3 Cutting edge condition post grinding

percentage of the deposited heat energy dissipates from the surface into the workpiece. This causes a fusion zone, and hence an undesirable surface integrity, e.g. changes of the mechanical properties of the workpiece [9].

The preparation of the cutting edge was carried out on uncoated cemented carbide tools. The unprepared cutting edges of these indexable inserts have a cutting edge radius of $r_ß = 7$ µm. The cutting edges are non-uniform prior to laser preparation as the macro geometry of the indexable inserts was generated through grinding (Fig. 3).

To adjust the cutting edges relative to the laser beam, a five-axis-positioning system with three linear axes and two rotary axes was used. This allows the laser beam to be focused along the entire cutting edge length. Furthermore, the scanning line of the laser beam could be adjusted parallel to the cutting edges. The cutting edges are inclined at 36° in the clamping device to ensure a uniform ablation on both the rake and the flank-face. The angle of 36° is consistent with the bisecting line of the wedge angle of the indexable inserts.

Cutting edge radii $r_ß$ and roughness of the cutting edges S were measured using a digital fringe projection system. The micro geometry of a separate cutting edge was determined at four identical measurement areas along the entire length of the cutting edge. The cutting edge radius and the roughness of the cutting edge are based on the mean value of these four measurement areas. Furthermore, the uniformity of the cutting edge radius along the entire length of the cutting edge can be evaluated using this measurement procedure.

3.1 Scanning strategy and input parameters of the laser system

To manufacture defined cutting edge radii, a laser processing area was defined along the cutting edge of width 300 µm perpendiculars to the cutting edges. Within this area several parallel scan lines are necessary for a extensive ablation. The laser source emits radiation from the start to the end of the scan line for the specified scanning strategy. Once the laser beam reaches the end of the scan line, radiation emission is stopped until the laser beam is positioned at the beginning of the next scan line.

Four relevant input parameters of the laser system need to be determined to generate a defined cutting edge radius.

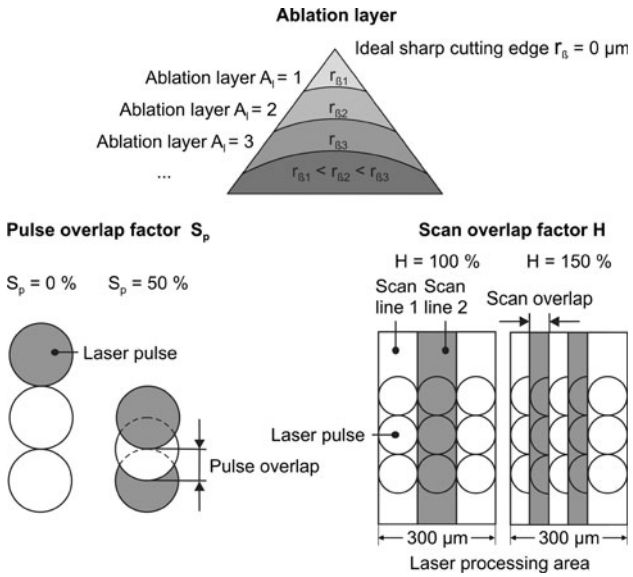

Fig. 4 Relevant input parameters of the laser system

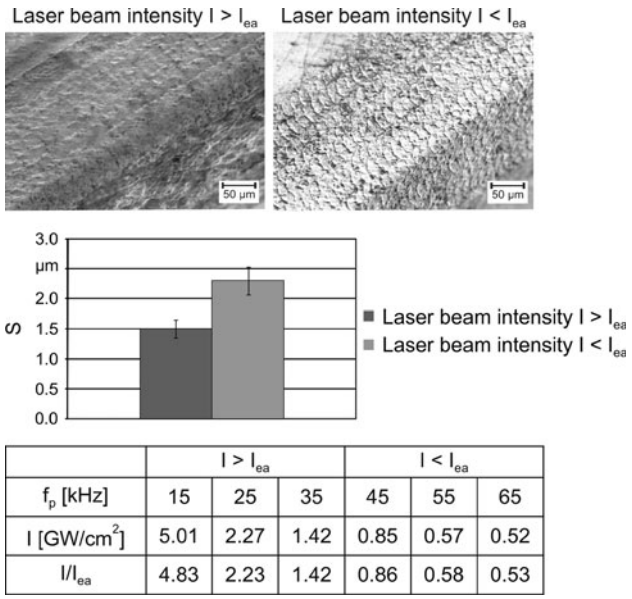

	I > I_{ea}			I < I_{ea}		
f_p [kHz]	15	25	35	45	55	65
I [GW/cm^2]	5.01	2.27	1.42	0.85	0.57	0.52
I/I_{ea}	4.83	2.23	1.42	0.86	0.58	0.53

Fig. 5 Cutting edge roughness S in relation to the laser beam intensity

These are the pulse frequency f_p, the pulse overlap factor S_p, the scan overlap factor H and the number of ablation layers A_l (Fig. 4). The pulse frequency describes the reciprocal value of the time between two pulse peaks. The pulse overlap factor specifies the overlap of sequential laser pulses, whereas the scan overlap factor defines the overlap of scan lines arranged in parallel. The pulse frequency and the pulse overlap factor determine the amount of ablated material in a scan line. The ablated material in an ablation layer is the sum of the ablated material from each scan line in the ablation layer.

Direct input parameters of the marking laser are the pulse frequency f_p, the number of ablation layers A_l, the scanning speed v_f, and the scan overlap factor H. Therefore, the pulse overlap factor S_p (Eq. 1) has to be indirectly adjusted by adjusting the scanning speed, the spot diameter and the pulse frequency.

$$S_p = 1 - \frac{v_f}{d\, f_p} \tag{1}$$

d, Spot diameter; f_p, Pulse frequency; S_p, Pulse overlap factor; V_f, Scanning speed

3.2 Threshold for laser sublimation

In order to vaporize the workpiece material, the intensity of the laser beam I (laser power per unit area) must exceed the threshold for laser sublimation I_{ea}. The intensity of the laser beam I is influenced mainly by the pulse frequency which determines the pulse peak power. Therefore, the estimation of the threshold for laser sublimation limits the applicable pulse frequencies for ablation. I_{ea} can be estimated with the following equations (Eq. 2, Eq. 3, Eq. 4) [9].

$$I_{ea} = \frac{2\lambda\sqrt{2\pi}}{Ad\,\arctan\sqrt{\frac{32\chi\tau_p}{d^2}}} T_e + \rho H_e v_b \tag{2}$$

$$v_b = \frac{1}{s_m}\chi \ln\left(\frac{T_e - T_o}{T_m - T_o}\right) \tag{3}$$

$$s_m = \frac{\lambda(T_e - T_m)}{IA} \tag{4}$$

A, Absorption coefficient; d, Spot diameter; He, Enthalpy of vaporization; I, Laser beam intensity; I_{ea}, Threshold for laser sublimation; S_m, Fusion phase thickness; T_o, Workpiece temperature; T_e, Vaporization temperature; T_m, Fusion temperature; V_b, Melt front velocity; λ, Thermal conductivity; χ, Thermal diffusivity; τ_p, Pulse duration; ρ, Density

For pulse frequencies higher than 40 kHz the laser beam intensity decreases below the threshold for laser sublimation. Consequently, pulse frequencies of more than 40 kHz cannot be used for cutting edge preparation. The estimate of the minimal required intensity of the laser beam for sublimation can be verified by varying the pulse frequency. Therefore, three lower, and three higher laser beam intensities than the calculated I_{ea} have been used for cutting edge preparation. With laser beam intensities lower than the determined I_{ea}, the amount of melted material increases and remains at the cutting edge (Fig. 5), and the roughness of the cutting edge S increases. With intensities higher than the determined I_{ea} the desired laser ablation and roughness was observed. These investigations confirmed the minimal laser beam intensity calculated for sublimation.

3.3 Effect of input parameters on cutting edge radius and cutting edge roughness

The impact of the relevant input parameters on the resulting cutting edge radius needs to be investigated when a defined cutting edge radii is to be generated. Therefore, uncoated, unprepared indexable inserts with a cutting edge radius of $r_ß = 7$ µm were used for the preparation of cutting edges. Each relevant input parameter was adjusted separately within a single ablation layer. The influence of the relevant input parameters on the cutting edge radius is detailed in Fig. 6.

The pulse overlap factor has the greatest influence on the cutting edge radius. Increasing the pulse overlap factor causes a rise in the cutting edge radius. This can be attributed to the increasing number of pulse hits and hence an increase in the deposited energy per unit area. The scan overlap factor has an insignificant influence on the cutting edge radius. Variation of the pulse frequency shows no clear effect. The cutting edge radius is almost constant for pulse frequencies of 25–40 kHz due to the minimal differences in the laser beam intensities. For pulse frequencies of 5–20 kHz the generated cutting edge radii decrease as the pulse frequency rises, because the laser beam intensities are consequently decreasing.

Furthermore, the influence of the pulse frequency, the scan overlap factor, and the pulse overlap factor on the cutting edge roughness is investigated in detail. In order to do this, unprepared cutting edges with comparable values of initial cutting edge roughness were used. The preparation of the cutting edges was performed by the removal of one ablation layer using different input parameters. The results are displayed in Fig. 7. A scan overlap factor of 133%, and pulse overlap factors of 30 and 60% result in a minimum cutting edge roughness. With regards to pulse frequencies, minimal cutting edge roughness can be achieved using pulse frequencies of 20–30 kHz. In summary, values for the roughness of cutting edges of

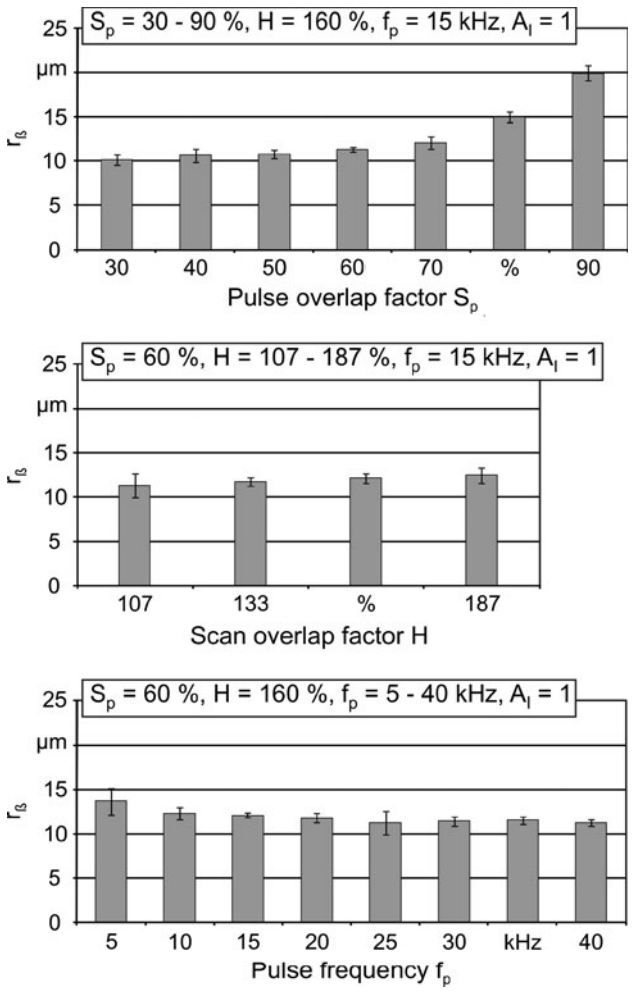

Fig. 6 Influence of pulse frequency, pulse and scan overlap factor on cutting edge radius

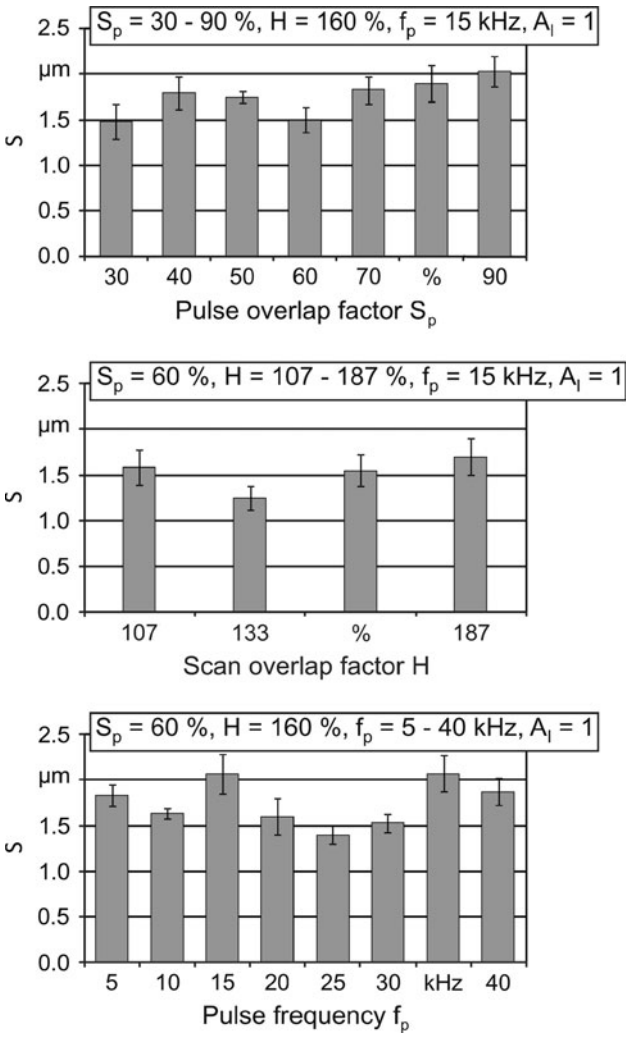

Fig. 7 Influence of input parameters on cutting edge roughness S

approximately 1.5 µm can be generated using the laser preparation when appropriate input parameters are used.

The results depicted in Figs. 6 and 7 focus on both the cutting edge radius and the cutting edge roughness when one ablation layer is removed from an unprepared cutting edge. For both a cutting edge radius larger than 14 µm and an appropriate cutting edge roughness, more than one ablation layer is required.

In order to reduce the processing time, a roughing and finishing process is preferable. As depicted in Fig. 6, the cutting edge radius is influenced mostly by the pulse overlap factor. A roughening process can be implemented using multiple pulse hits per unit area. However, an increasing number of pulse hits per unit area still causes an increase in the cutting edge roughness due to the prolonged interaction time of the laser beam on a specified unit area. This results in more material being melted and remaining on the cutting edge. For this reason it can be concluded that a roughing process can be applied for the preparation of cutting edges if the roughness of the cutting edge surface can be decreased within one ablation layer. In order to investigate the possibility of a finishing operation, a cutting edge was prepared by roughing ($f_p = 20$ kHz, $S_p = 90\%$, $H = 187\%$, $A_l = 2$). The reduction of the cutting edge roughness within one ablation layer was then tested. The results, displayed in Fig. 8, confirm that surface finishing with one ablation layer is possible. For the surface finishing of the cutting edge a scan overlap factor of 133%, a pulse frequency of 20–30 kHz and a pulse overlap factor of 50–70% should be used.

3.4 Generation of cutting edge radii

Cutting edge radii of approximately 9–47 µm can be generated using the identified relevant input parameters (chapter 3.3). Uniformity variation of the cutting edge radius along the entire cutting edge length is below one micrometer. The machining accuracy for generating a specified cutting edge radius varies from 0.4 to 1.3 µm. This variation can be explained by the number of ablation layers required for manufacturing of a specified cutting edge radius. More than one ablation layer has to be removed to generate cutting edge radii greater than 14 µm with the appropriate cutting edge roughness. The total machining accuracy is an accumulation of the accuracy of each individual ablation layer. The higher the number of applied ablation layers, the lower the overall machining accuracy. The laser preparation of cutting edges, however, achieves sufficient accuracy to manufacture defined cutting edge radii. The preparation time for a single cutting edge is progressively increasing with increasing cutting edge radius. Cutting edge radii of $r_\beta = 9$ µm, $r_\beta = 14$ µm, $r_\beta = 28$ µm and $r_\beta = 47$ µm are generated in approximately 0.3 s, 1.7 s, 3.6 s respectively, 10 s. Scanning electron microscopy (SEM) images and metallographic sections show two cutting edge radii ($r_\beta = 20$ µm and $r_\beta = 47$ µm) in Fig. 9. The images in Fig. 9 confirm that the desired cutting edge radii can be generated with the described scanning strategy (chapter 3.1) without a remarkable surface alteration.

4 Tool life experiment

To analyze the capability of a low-cost marking laser for cutting edge preparation three different cutting edge radii were used in a face milling operation (Fig. 10). Unprepared cutting edges with the cutting edge radius $r_\beta = 7$ µm as well as prepared indexable inserts with cutting edge radii of $r_\beta = 14$ µm and $r_\beta = 28$ µm were used. The experiments were carried out on a five-axis drilling-and-milling machining center without coolant. The material of the workpiece used was cast iron. Passive and active forces, surface roughness, and flank wear were measured in order to study the influence of the cutting edge radius on the

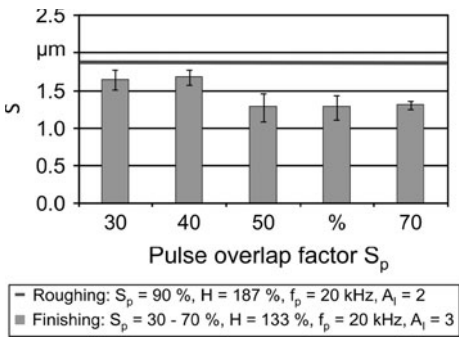

Fig. 8 Surface finishing with one ablation layer

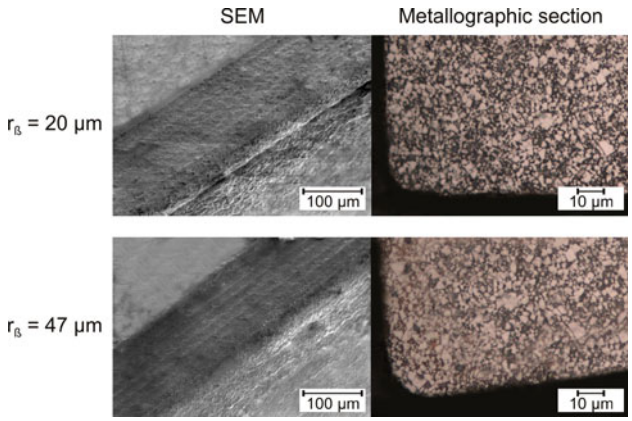

Fig. 9 Laser prepared cutting edge radii

Manufacturing process	Tool macro geometry
Face milling	ODMW 120408
Cutting condition	**Tool micro geometries**
Cutting speed: 160 m/min	r_β = 7 µm
Feed per tooth: 0.1 mm	r_β = 14 µm
Depth of cut: 2.5 mm	r_β = 28 µm
Width of cut: 36 mm	
Workpiece material	**Cutting material**
Cast iron	Uncoated cemented carbide
Coolant	
None	

Fig. 10 Experimental setup

machining process. Forces were measured during the process whereas surface roughness and flank wear were investigated following defined path lengths due to primary motion l_c. A three-component-dynamometer was used and the average values for passive and active forces were determined in order to evaluate the forces. Average surface roughness R_a was detected by a tactile measurement system perpendicular to the primary motion. Flank wear was analyzed with a reflected-light microscope using the maximum wear at the straight part of the cutting edge VB_{max}. Tool life criteria were defined as either a maximum wear at the straight part of the cutting edge of 300 µm, or cutting edge chipping, or a maximum path length due to primary motion of 1,250 m.

4.1 Experimental results

The experimental investigations reveal that tool life can be increased through the use of laser preparation of cutting edges. The laser prepared cutting edges achieve the tool life criterion of $l_c = 1{,}250$ m path length due to primary motion while the unprepared cutting edges fail after $l_c = 760$ m due to chipping of the cutting edges (Fig. 11). The condition of the cutting edges after achieving the tool life criterion is illustrated in Fig. 12. Reflected-light microscope images demonstrate built-up edges at each cutting edge leading to a non-uniform cutting edge. Considering these non-uniform cutting edges due to the built-up edges, cutting edge chipping is only observable at the unprepared cutting edges. The unprepared cutting edges reveal the highest VB_{max} during the complete investigations. In contrast, laser prepared cutting edges with $r_\beta = 28$ µm show minimum flank wear (Fig. 11). The short tool life travel path of the unprepared cutting edges can be attributed to both the non-uniform micro geometry of the cutting edges and to the low cutting edge stability of small cutting edge radii in general. The non-uniform micro geometry of the unprepared cutting edges originates from the superficial defects occurring during grinding for the manufacture of the tool macro geometry [12]. These superficial defects decrease the cutting edge stability. In addition, chip deformation occurs on the sharp tip of the cutting edge when small cutting edge radii are used for machining. Therefore, high pressures and temperatures occur at the sharp tip of the cutting edge [13]. In summary, the stability of cutting edges increases with the increase of cutting edge radii within the scope of the investigated cutting edge radii.

Machined workpieces using indexable inserts with prepared cutting edges show better surface qualities compared to workpieces machined with unprepared cutting edges after $l_c = 350$ m (Fig. 11). The workpiece surface roughness increases almost continuously with rising path length due to primary motion when unprepared cutting edges are used for machining. In contrast, surface roughness shows no significant increase during machining with prepared cutting edges. Since surface roughness is influenced by the condition of the tool micro geometry, it can be concluded that the prepared cutting edges show no significant cutting edge chipping (Fig. 12) when the tool life criterion of $l_c = 1{,}250$ m is achieved.

The indexable inserts with a cutting edge radius of 28 µm reveal both the highest passive, and the highest active force at a path length due to primary motion of $l_c < 20$ m (Fig. 11). This can be attributed to the major material deformation at the front of the cutting edge due to the larger negative effective rake angle compared to $r_\beta = 14$ µm and $r_\beta = 7$ µm. Therefore, the material undergoes greater deformation prior to the transition from base material to chips and a greater percentage of the base material is pushed under the cutting edge. Furthermore, the contact surface between tool and workpiece, and hence the contact pressure per unit area in the contact surface increases with rising cutting edge radius.

Both passive and active forces were similar for cutting edge radii of 7 and 14 µm in the preliminary stages of the investigation despite the above mentioned effects. A possible explanation for the fact that the forces occurring at $r_\beta = 7$ µm and $r_\beta = 14$ µm were similar could be the major tool wear on the 7 µm cutting edge radius indexable insert which led to the active and passive forces being almost equal.

All cutting edge radii used show an increase in both passive and active forces with an increase in path length due to primary motion. The strongest increase of both

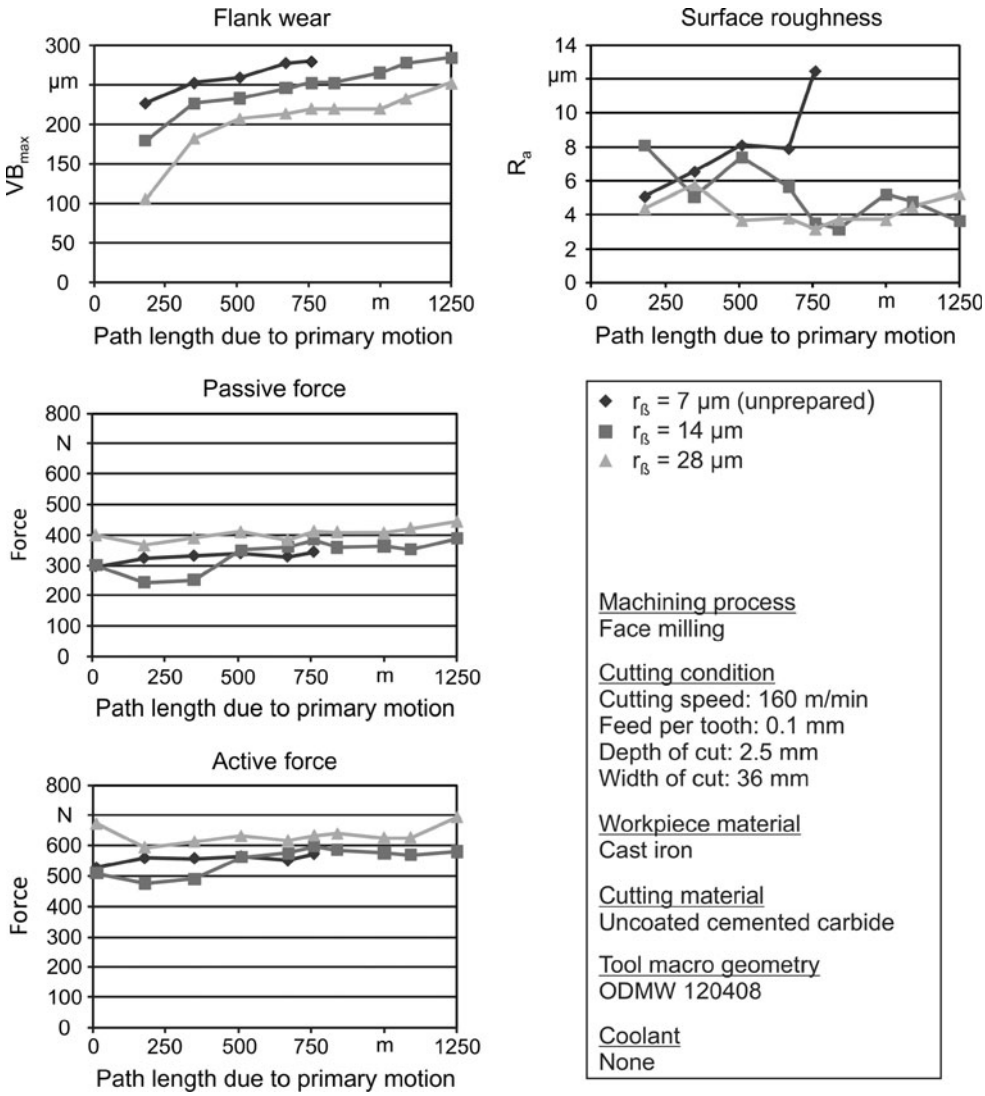

Fig. 11 Experimental results of the face milling process

passive and active forces was observed for the indexable inserts with a cutting edge radius of $r_ß = 14$ µm (Fig. 11). In contrast to this, the lowest increase of both active and passive forces was shown when machining with a cutting edge radius of $r_ß = 28$ µm. This is probably due to lower tool wear in general, and the consequent lower change in cutting edge micro geometry due to tool wear (Fig. 12). In summary, it can be concluded that the cutting edge with $r_ß = 28$ µm demonstrates the highest cutting edge stability.

5 Conclusions

In this paper, cutting edge preparation was successfully performed using a low-cost marking laser. The applied preparation procedure allows a cutting edge radius of 9–47 µm to be generated. The machining accuracy varies from 0.4 to 1.3 µm. Values for the cutting edge roughness of approximately 1.5 µm can be generated. The maximum preparation time for a single cutting edge is approximately 10 s. In a face milling process unprepared cutting edges with $r_ß = 7$ µm and prepared cutting edges ($r_ß = 14$ µm, $r_ß = 28$ µm) were used. Both an improvement of tool life and machining quality was observed when laser preparation of cutting edges was used. The unprepared cutting edges failed after $l_c = 760$ m due to chipping of cutting edges whereas the laser prepared cutting edges achieved the defined maximum path length due to primary motion of 1,250 m. Within the scope of the cutting edge radii used, the performance of the indexable inserts increased with a greater cutting edge radius. Therefore, it can be concluded that cutting edge preparation using a low-cost marking laser is an alternative to conventional preparation methods such as brushing or blasting. In order to gain better knowledge with regard to the cutting tool performance, the

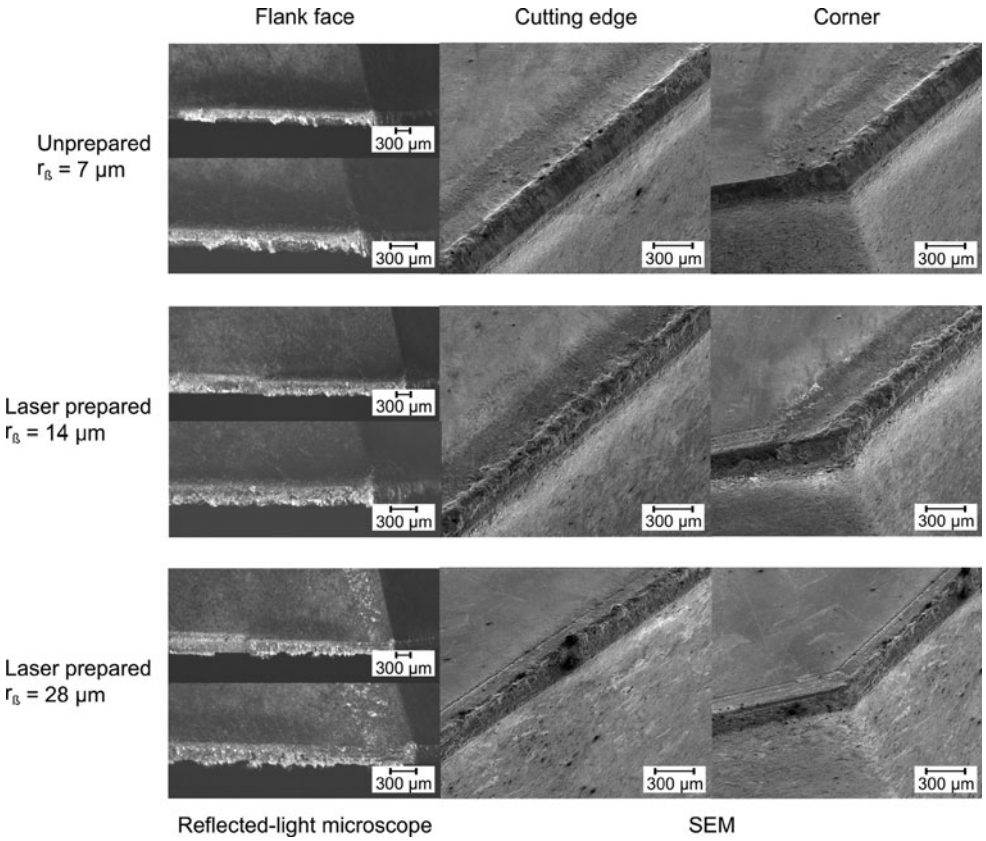

Fig. 12 Tool condition when reaching tool life criterion

influence of laser machining to the surface layer of the cutting material needs to be investigated in detail in further investigations.

References

1. Byrne G, Dornfeld D, Denkena B (2003) Advancing cutting technology. Annals of the CIRP 52(2):483–507
2. Biermann D, Weinert K, Terwey I, Denkena B, Haubrock J (2009) Vorteile durch Verrundung. Einsatzverhalten komplexer Werkzeuge mit präparierten Schneidkanten. WB Werkstatt und Betrieb 142(11):36–40
3. Shaffer B (2005) Advances in edge preparation offer production advantages. Tool Prod 71:14–16
4. Byelyayev O (2008) Erhöhung der Leistungsfähigkeit von HSS-Spiralbohrern durch Einsatz der magnetabrasiven Bearbeitung. Dissertation, University Magdeburg
5. Denkena B, Weinert K, Friemuth T, Spengler C, Schulte M, Kötter D (2003) Kantenpräparation an Hartmetall Werkzeugen–Einfluss der Prozessparameter beim Strahlen und Bürsten. VDI-Z Special Werkzeuge 3:51–54
6. Denkena B, Kramer N, Siegel F, Kästner J (2007) Methoden zur Präparation von Zerspanwerkzeugen: Leistungsoptimierung an der Schneidkante. VDI-Z Special Werkzeuge 8:24–26
7. Ostendorf A, Kulik C, Siegel F (2004) Cutting tools preparation using short pulse lasers. LANE, Laser Assisted Net Shape Engineering 4:681–690
8. Rech J, Yen Y C, Hamadi H, Altan T, Bouzakis K D (2004) Influence of cutting edge radius of coated tool in orthogonal cutting of alloy steel. In: Proceedings of the 8th international conference on numerical methods in industrial forming processes 712:1402–1407
9. Rech J (2005) Influence of cutting edge radius on the wear resistance of PM-HSS milling inserts. Wear 259:1168–1176
10. Denkena B, Friemuth T, Fedorenko S, Groppe M (2002) An der Schneide wird das Geld verdient. Werkzeugtechnik+Verfahren 30(12):24–26
11. Kordt J (2007) Konturnahes Laserstrahlstrukturieren für Kunststoffspritzgießwerkzeuge. Dissertation, RWTH Aachen
12. Tönshoff HK, Friemuth T (1999) Effects of grinding on the performance of cutting tools. Prod Eng 6(2):9–12
13. Guter T (2009) Kantenpräparation an Wendeschneidplatten, Kantenpräparation an Wendeschneidplatten–der Schlüssel zu leistungsstarker Zerspanung. In: Tikal F Schneidkantenpräparation, Ziele, Verfahren und Messmethoden. Kassel, University press, pp 71–86